Human Molecular Genetics, 2009, Vol. 18, No. 15 **2791–2801**
doi:10.1093/hmg/ddp214
Advance Access published on May 5, 2009

Defective pulmonary vascular remodeling in *Smad8* mutant mice

Zheng Huang[1], Degang Wang[1], Kaori Ihida-Stansbury[2], Peter Lloyd Jones[2] and James F. Martin[1,*]

[1]Institute of Biosciences and Technology, Texas A&M System Health Science Center, 2121 W. Holcombe Blvd, Houston, TX 77030, USA and [2]Institute for Medicine and Engineering, Department of Pathology and Laboratory Medicine, University of Pennsylvania, Philadelphia, PA, USA

Received February 24, 2009; Revised April 21, 2009; Accepted May 1, 2009

Pulmonary artery hypertension (PAH), a progressive, lethal condition that results in pathologic changes in the pulmonary arterial tree, eventually leads to right heart failure. Work identifying mutations in the Type II Bone morphogenetic protein (Bmp) receptor, *BmpRII*, in families with PAH has implicated Bmp-signaling in the pathogenesis of PAH. However, the effectors downstream of *BmpRII* in PAH remain unclear since *BmpRII* signals via Smad-dependent and independent mechanisms. We investigated *Smad8* function, a divergent receptor regulated Smad downstream of Bmp-signaling, using gene targeting in mice. We show that *Smad8* loss of function in adults resulted in characteristic changes in distal pulmonary arteries including medial thickening and smooth muscle hyperplasia that is observed in patients with PAH. *Smad8* mutant pulmonary vasculature had upregulated Activin/Tgfβ signaling and pathologic remodeling with aberrant Prx1 and Tenascin-C expression. A subset of *Smad8* mutants had pulmonary adenomas uncovering a function for *Smad8* in normal growth control. These findings implicate *Smad8* in both pulmonary hypertension and lung tumorigenesis and support *Smad8* as a candidate gene for PAH in humans.

INTRODUCTION

The Bone morphogenetic protein family *(Bmp)* of growth factors is a subgroup in the Tgfβ super family of signaling molecules (1). The Bmp ligands are an evolutionarily conserved group that signal via a heteromeric complex composed of type I and type II receptors. Upon activation, the serine-threonine kinase type I receptor phosphorylates one of the Bmp receptor regulated Smads (R-Smads): *Smad1*, *Smad5* or *Smad8* (2). After phosphorylation, the R-Smad is released from the receptor complex and associates with the common Smad4 to form a trimeric complex composed of two R-Smads and Smad4. This Smad complex then translocates to the nucleus to regulate gene expression in combination with other cofactors. In addition to the canonical Smad-mediated pathways, Bmp-signaling has been shown to activate Map Kinase-mediated effector pathways (2). More recent experiments, indicating a role for Bmp-signaling in microRNA (miRNA) regulation, have revealed further complexity in Bmp-regulated effectors (3).

In addition to a critical role in normal embryogenesis, Bmp-signaling has been implicated in inherited disorders that involve defective vascular remodeling and cellular growth and differentiation (4,5). Human genetic studies identified loss-of-function mutations in the type II Bmp receptor *(BmpRII)*, in families with pulmonary artery hypertension (PAH) (6). Idiopathic or primary PAH primarily involves the small, distal pulmonary arteries that show muscular hypertrophy and intimal hyperplasia (7). This work uncovered a role for Bmp-signaling in pulmonary vasculature homeostasis (6,8,9). Recent data also indicate that one family with PAH contains a truncating mutation in *Smad8* suggesting a role for *Smad8* in the pathogenesis of familial PAH (10).

In addition to PAH, loss-of-function mutations in the type I Bmp receptor, *Bmpr1a*, are known to result in juvenile polyposis syndrome (JPS), a hamartomatous condition that results in benign growths containing severely disorganized intestinal tissue. Importantly, patients with JPS and JPS animal models have a high likelihood of developing colon cancer indicating a role for Bmp-signaling in regulating epithelial growth

*To whom correspondence should be addressed.Tel: +1 7136777558; Fax: +1 7136777512; Email: jmartin@ibt.tamhsc.edu

(11,12). Loss-of-function mutations in the Tgfβ pathway components, endoglin and ACVRL1 (ALK1) cause hereditary hemorrhagic telangiectasia that results in pulmonary arteriovenous malformations and other vascular dysplasias (4).

In addition to loss of function, gain-of-function mutations in Bmp-signaling components also result in human disease. A gain-of-function mutation in the type I receptor ACVR1 (also called Alk2) results in fibrodysplasia ossificans progressiva (13). This is a fascinating syndrome in which ectopic soft tissue ossification occurs in concert with inflammatory stimuli. This phenotype suggests an *in vivo* link between Bmp and stress-regulated signaling that has been previously observed in tissue culture cells (14).

Other *in vivo* experiments provide insight into Bmp-signaling in vascular development. We previously found that *Bmp4* was required for remodeling of branchial arch arteries during mouse development (15). Moreover, work investigating the function of the Bmp R-Smads, *Smad1* and *Smad5*, revealed important functions for these genes in early development (16–20). *Smad1* and *Smad5* mutant mice were embryonic lethal with defects in the allantois resulting in abnormal placentation. *Smad5* was also shown to be critical for early events in the development of left right asymmetry. Vascular abnormalities within the embryo proper were also observed in both *Smad1* and *Smad5* mutant embryos (16–20). Despite these severe embryonic phenotypes, the *Smad1* and *Smad5* mutant mice survived longer than mice that were mutant for *Bmpr1a* and *BmpRII* likely as a result of redundancy between the Smad family members. As noted earlier, it is also conceivable that Smad-independent signaling may play a role in the *Bmpr1a* and *BmpRII* mutant phenotypes (3,21–23).

Previous work indicated that *Smad8* has only minor functions in development due in part to redundancy with *Smad1* and *Smad 5* (23,24). Because little is known about the function of *Smad8* and Bmp-signaling in the adult, we investigated *Smad8* in adult mice using a loss-of-function approach. Our data indicate that *Smad8*, although dispensable for embryogenesis, has an important role in pulmonary vasculature maintenance. In *Smad8* mutant mice, pathologic changes consistent with PAH were observed in the distal pulmonary vasculature. These pathologic changes were associated with defective vascular remodeling with aberrant Tenascin-C (TN-C) and Prx1 expression. We also found increased Activin and/or Tgfβ signaling activity, as determined by phospho-Smad2 (P-Smad2) expression, in *Smad8* mutant vessels. Additionally, a subset of *Smad8* mutants developed lung adenomas implicating *Smad8* in lung neoplasia. Taken together, our data provide new insight into *Smad8* function and the genetic pathways involved in PAH.

RESULTS

Generation of the $Smad8^{ex4,5}$ and $Smad8^{lacZ}$ alleles

To study the *Smad8* function, we generated the $Smad8^{ex4,5}$ and $Smad8^{lacZ}$ alleles using gene targeting in embryonic stem cells (Materials and Methods and Fig. 1). In the $Smad8^{flox}$ allele, exons 4 and 5 were flanked by two LoxP sites with a Frt flanked Pgk Neomycin resistance cassette located 3′ of exon 5 (Fig. 1A–E). We used a germline cre deletor strain to remove exons 4 and 5 and generate the $Smad8^{ex4,5}$ allele. The *Smad8* exons 4 and 5 encode a major part of the Smad8 MH2 domain and contain essential motifs such as the receptor binding domain and the phosphorylation site, with the SSXS motif. Therefore, the $Smad8^{ex4,5}$ allele would be predicted to be a null allele. This idea is supported by experiments performed with *Smad5* in which the C-terminal deletion gave nearly identical phenotypes to a deletion of exon 1 and the initiator methionine (16,18).

We also generated a $Smad8^{lacZ}$ allele by introducing an IRES LacZneomycin cassette into exon 4 of *Smad8* (Fig. 1F–I). By marking cells that are fated to express *Smad8*, the $Smad8^{lacZ}$ allele would provide insight into the spatio-temporal transcriptional regulation of *Smad8*. Moreover, disruption of exons 4 and 5 in the $Smad8^{lacZ}$ allele would be predicted to give a similar functional outcome to the $Smad8^{ex4,5}$ allele.

To determine whether the $Smad8^{lacZ}$ allele was a null allele, we performed immunostaining with an antibody against Smad8 that recognizes an epitope in the linker region that is still present in the $Smad8^{lacZ}$ allele. Because we found that *Smad8* was highly expressed in the prostate epithelium in adult mice (see below), we used sections through prostate and performed double-labeling by staining for LacZ activity to show cells that are transcribing *Smad8* and Smad8 immunostaining to detect Smad8 protein (Fig. 1J–M). In $Smad8^{lacZ}$ heterozygous prostatic epithelium, Smad8 protein was detected in the cytoplasm of LacZ-positive luminal epithelial cells (Fig. 1J and K). The $Smad8^{lacZ}$ −/− luminal prostatic epithelium was positive for LacZ activity but immunoreactivity with the Smad8 antibody was absent (Fig. 1L and M). Taken together, these data support the conclusion that the $Smad8^{lacZ}$ allele is null.

Analysis of the $Smad8^{lacz}$ allele indicates that *Smad8* is expressed in discrete regions during embryogenesis

We used LacZ staining to detect β-galactosidase expressed from the $Smad8^{lacZ}$ knock-in allele at embryonic stages. LacZ activity was found in discrete locations in embryos from 11.5 to 13.5 days post coitum (dpc), indicating that *Smad8* transcription is developmentally regulated (Fig. 2). At 11.5 and 12.5 dpc, LacZ expression was detected in the cardiac outflow tract (OFT), in both the myocardium and cushion mesenchyme (Fig. 2A–D). LacZ was also detected in the atrioventricular (AV) cushion mesenchyme (Fig. 2D). Both the OFT and AV cushions require Bmp-signaling for normal development (15,25–27).

From 12.5 to 16.5 dpc, LacZ activity was also detected in developing skeletal structures (Fig. 2E–H). LacZ was found in the cartilaginous and bony elements of the forming long bones of the limb (Fig. 2 E and G), in membranous bones of the craniofacial skeleton (Fig. 2F), and in the developing ribs (Fig. 2H). We also detected LacZ activity in the tracheal rings of the upper airway, a Bmp4 sensitive structure [Fig. 2I; (28,29)]. In the forming guts, LacZ was detected at the junction between the pylorus and duodenum at 11.5 and 13.5 dpc (Fig. 2J and K), forming a sharp ring of expression at the junction of the pyloris of the stomach and duodenum. Bmp-signaling is known to specify the duodenal-pyloric

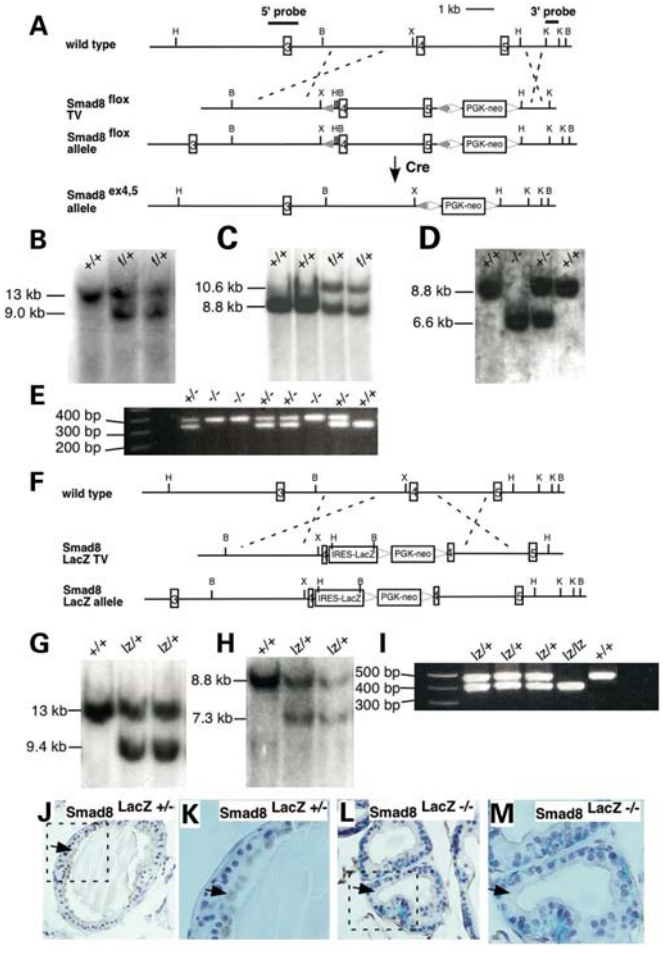

Figure 1. Targeting strategies to generate the *Smad8*^{ex4,5} and *Smad8*^{LacZ} alleles. (**A**) Schematic representation of partial *Smad8* endogenous locus and targeting strategy of generating *Smad8 ex4,5* allele. External probes are represented with thick lines. In the targeting vector, exons 4 and 5 are flanked by LoxP sites (filled triangle). The Frt-flanked PGK-neo follows the 3′ LoxP site. Homologous recombination produced *Smad8*^{flox} allele and Cre-mediated excision of exons 4 and 5 yielded the *Smad8*^{ex4,5} allele. (**B**–**E**) Southern and PCR assays for *Smad8 ex4,5* allele. (B) Southern blotting of *Hin*d III digest DNA from targeted ES cells using 5′ external probe. The size of the wild-type band is 13 kb, while 9.0 kb for *Smad8*^{flox} (f) allele. (C) Southern blotting of *Bam*H I digest DNA from progeny of the cross between *Smad8*^{flox} chimera and C57Bl/6J. 8.8 kb wild-type band and 10.6 kb band for *Smad8*^{flox} (f) allele were detected using 3′ external probe. (D) Southern blot for cre excision event using 3′ external probe. Deletion of exons 4 and 5 yielded 6.6 kb band for *Smad8*^{ex4,5} (−) allele. (E) PCR genotyping of mice from *Smad8*^{ex4,5} intercross. Mutant band is 410 bp and wild-type band is 320 bp. (**F**) LacZ knock-in strategy in Smad8 locus. The IRES-LacZ followed by LoxP-flanked PGK-neo was placed in the middle of exon 4. Homologous recombination resulted in the Smad8^{lacZ} allele. (**F**–**I**) Southern and PCR assays for *Smad8*^{lacZ} (lz) allele. (G) Southern blotting of *Hin*d III digest DNA from targeted ES cells. *Smad8*^{lacZ} allele yields 9.4 kb band using 5′ external probe. (H) Southern blotting of *Bam*H I digest DNA from embryos collected from the cross between *Smad8*^{lacZ} chimera and C57Bl/6J. 7.3 kb was detected from *Smad8*^{lacZ} allele. (I) PCR genotyping of embryos from *Smad8*$^{lacZ\ /+}$ intercross. The wild-type band is 470 bp in length, and the 370 bp band detects *Smad8*^{lacZ} allele. (**J** and **K**) Smad8 protein was detected in the luminal cytoplasm of epithelial cells in the *Smad8*^{lacZ} +/− prostate (arrow). (K) is higher magnification of boxed area in (J). (**L** and **M**) In *Smad8*^{lacZ} −/− prostate, Smad8 protein was not detected. Note the strong nuclear LacZ staining denoting cells that are actively expressing Smad8. (M) is higher magnification of boxed area in (L). B, *Bam*H I; H, *Hin*d III; K, *Kpn* I; X, *Xho* I.

junction (30,31). *Smad8*^{lacZ} also directed LacZ activity in the genital tubercle and adrenal glands (Fig. 2L and M). Together, these data indicate that *Smad8* is expressed at embryonic sites where Bmp-signaling is known to be important.

Smad8 expression in postnatal and adult mice

In adult mice, we found that the *Smad8*^{lacZ} allele directed LacZ expression in the luminal epithelium of the prostate (Figs 1J–M and 3A and B). While the wild-type prostate had only low levels of background staining (Fig. 3A), we observed strong nuclear localized LacZ staining in the anterior, dorsal and lateral lobes of the *Smad8*^{lacZ} prostate (Fig. 3B). There was no LacZ activity in the ventral lobes of the prostate. In the gut, LacZ expression was detected in the stomach and the duodenum, with strongest expression in the proximal duodenum (Fig. 3C and D). There was only minimal background LacZ activity in wild-type controls (Fig. 3C).

Defective Bmp-signaling has been implicated in the etiology of familial pulmonary arterial hypertension (6,8). Interestingly, LacZ activity was detected in postnatal lungs of *Smad8*^{lacZ} +/− and *Smad8*^{lacZ} −/− mice. Expression reached a peak at 7 days post partum (P7) and was downregulated at later timepoints (Fig. 3E–G). Sections through P7 lungs revealed that LacZ activity was found throughout the parenchyma of the lung and in cells surrounding distal pulmonary vessels that most likely represent smooth muscle although further double labeling experiments are required to definitively address the Smad8-expressing cell type (Fig. 3H–K). Taken together, our data are consistent with previously published reports looking at embryonic expression and provide new insight into post-natal *Smad8* expression patterns (23).

Smad8^{lacz} mutants develop pulmonary vascular disease

Breeding experiments indicated that mice homozygous mutant for both the *Smad8*^{ex4,5} and *Smad8*^{lacZ} alleles were recovered at the normal Mendelian ratio at all stages examined (Tables 1 and 2). *Smad8* mutants had normal body size without gross abnormalities and were fertile. Histologic analysis of *Smad8*^{ex4,5} and *Smad*^{lacZ} homozygous mutant embryos at multiple stages failed to uncover anatomic abnormalities (not shown). These data indicate that *Smad8* loss of function is compatible with normal development and is consistent with a previous report describing a different *Smad8* allele that had a deletion of the first *Smad8* coding exon (23).

Since *Smad8* was dispensable for development, we investigated whether *Smad8* had a function in tissue homeostasis in adult mice. For the analysis of adult phenotypes, we focused on the *Smad8*^{lacZ} allele. We analyzed the lungs of *Smad8*^{lacZ} homozygous mutant mice and control mice by histology. Because of the firm connection of Bmp-signaling to pulmonary vascular disease and our observation that *Smad8* was expressed in the postnatal lung, we studied the *Smad8*^{lacZ} mutant lungs at multiple timepoints.

At 3 and 7 months of age, no lung pathology was observed in the *Smad8*^{lacZ} mutant mice ($n = 4$, not shown). However, beginning at 11.5 months of age, we observed pathologic

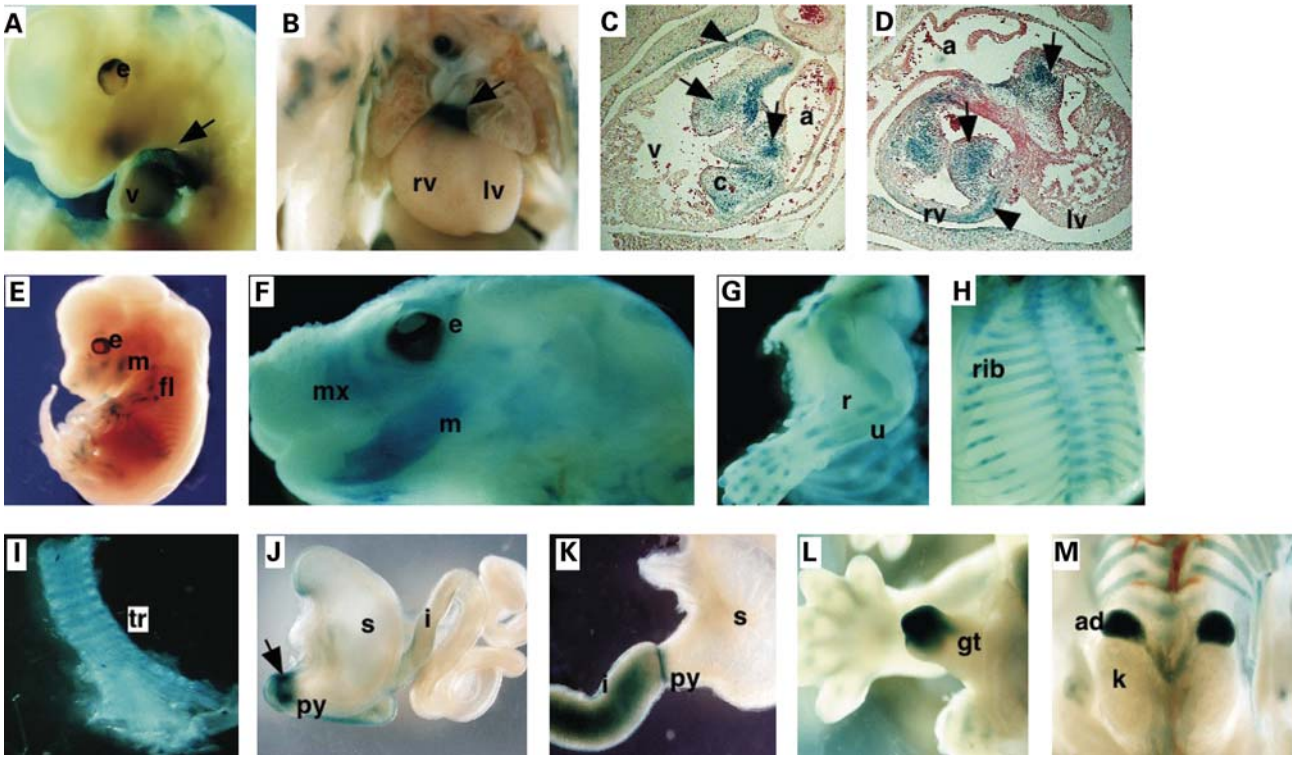

Figure 2. *Smad8*^{lacZ} expression pattern during embryogenesis. (**A** and **B**) LacZ staining at embryonic timepoints showed that *Smad8*^{lacZ} was expressed in the OFT of the heart (·) (**C** and **D**) Sections through 13.5 dpc hearts showing LacZ activity in the AV and OFT cushion mesenchyme (arrows) and myocardium (arrowheads). (**E**) *Smad8*^{lacZ} was expressed in the developing skeletal structures including the mandible and long bones (**E**–**G**) and developing ribs (**H**). LacZ activity was also found in the trachea (**I**). LacZ activity was detected in the gut: at 11.5 dpc in the pylorus (arrow) and the wall of duodenum (**J**) and in the pylorus and the duodenum at E13.5 (**K**). There was strong *Smad8*^{lacZ} expression in adrenal glands and the genital tubercle at E13.5 (**L** and **M**). a, atrium; c, cushion; e, eye; fl, forelimb; gt, genital tubercle; i, intestine; k, kidney; lv, left ventricle; m, mandible; mx, maxilla, py, pulorus; r, radius; rv, right ventricle; s, stomach; tr, trancha; u, ulna.

changes consistent with defective vascular remodeling in *Smad8*^{lacZ} −/− mice (Fig. 4A–C). The pathologic findings were consistent with what has been observed in human patients (7). Affected vessels were the distal pulmonary arterioles found at the lung periphery. Common findings included media hyperplasia with vessel occlusion and plexiform lesions (Fig. 4A–E). In addition, we commonly found an inflammatory monocytic infiltrate surrounding affected pulmonary vessels (Fig. 4C). We examined a total of 15 adult *Smad8*^{lacz} −/− mice and uncovered pathologic findings consistent with abnormal vascular remodeling such as media hyperplasia, occlusion and plexiform lesions in six mice (40%). It is notable that in the four *Smad8*^{lacZ} +/− controls that we examined, we observed limited evidence of vascular lesions in two mice. The changes were much less severe than in the homozygous mutants (Fig. 4F, data not shown). Abnormal vessels were observed in a few scattered areas and the media hyperplasia was mild. This is consistent with the dominant genetics observed in human patients with PAH (7).

Abnormal vascular remodeling in Smad8 mutants

Immunostaining with a smooth muscle actin antibody indicated that the cells within the media of abnormal vessels expressed smooth muscle markers suggesting abnormal vessel remodeling in the absence of *Smad8* (Fig. 4F–H). We performed PCNA staining on the *Smad8*^{laz} −/− vessels to determine whether there was aberrant cell cycle progression in the media of the affected pulmonary vessels. PCNA staining followed by cell counting to quantitate cell cycle progression in the *Smad8*^{laz} −/− spindle-shaped cells within the vessel media indicated that ∼50% were PCNA positive. However, cell counting and calculation of the proliferative index indicated that at the timepoints tested there was equivalent proliferation in the pulmonary smooth muscle of control and *Smad8* mutant vessels (Fig. 4I–L). This suggests that abnormal smooth muscle proliferation in the *Smad8* mutant vessels was a limited, acute event that was undetectable at the timepoints we studied. It is also possible that the *Smad8*^{laz} +/− mice that we used as controls for this experiment had upregulated cell proliferation, thereby diminishing the statistical power of this experiment. Further experiments with aged mice will be required to address this issue.

The extracellular matrix (ECM) glycoprotein, Tenascin-C (TN-C), is known to be upregulated in pathologically remodeling vessels of both clinical and experimental PAH (32–34). Moreover, the *Prx1* homeobox gene is required for normal pulmonary vascular development and is a direct transcriptional regulator of TN-C (34,35). Notably, *TN-C* and *Prx1* expression is silenced in the normal adult lung (34). We examined TN-C and Prx1 expression in *Smad8*^{lacZ} +/− and *Smad8*^{laz} −/− mutant lungs. In *Smad8*^{lacZ} +/− pulmonary

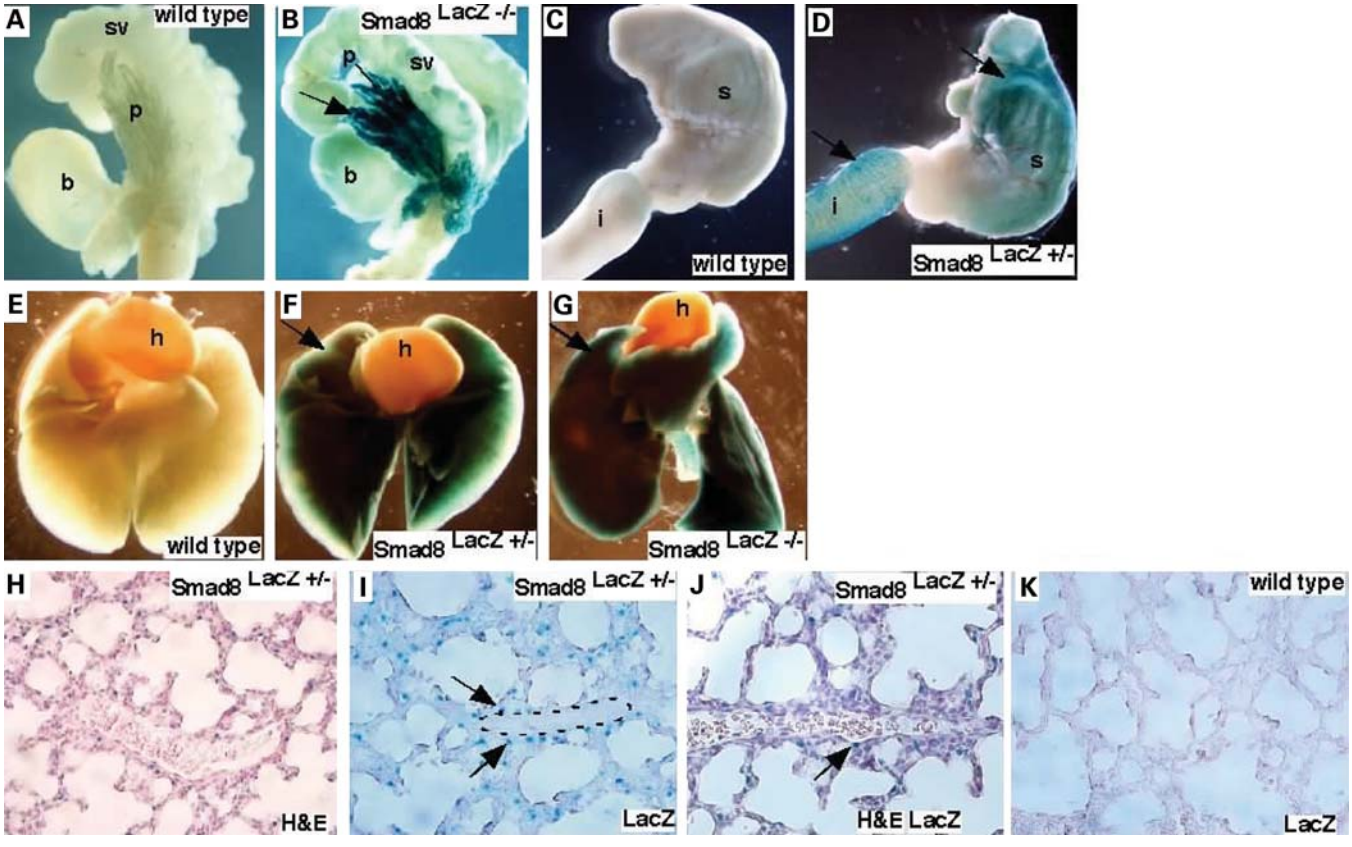

Figure 3. *Smad8*^{lacZ} expression pattern in postnatal tissues. (**A** and **B**) *Smad8*^{lacZ} expression was found in the prostate epithelium. (A) Wild-type control and (B) *Smad8*^{lacZ} $-/-$ indicated that Smad8 was highly expressed in anterior and dorsal-lateral prostate lobes. (**C** and **D**) LacZ activity was detected in the stomach and the proximal duodenum. (C) Wild-type control and (D) *Smad8*^{laZ} heterozygous tissues. (**E**–**G**) LacZ activity was detected in whole mount lungs from P7 mice. (**H**–**J**) Sections of P7 lungs indicate that Smad8 was expressed in the lung parenchyma and in cells surrounding pulmonary vessels [outlined in (I)]. (J) is a section stained with H&E and LacZ. The arrow indicates a Smad8 expressing cells adjacent to a distal pulmonary artery. (**K**) is a wild-type embryo used as a negative control for LacZ activity. B, bladder; h, heart; i, intestine; s, stomach; p, prostate; sv, seminal vesicle.

vessels, we found limited but detectable levels of TN-C and Prx1 indicating that Smad8 heterozygotes abnormally activate the Prx1-TN-C pathway (Fig. 4M and O). In *Smad8*^{lacZ} $-/-$ pulmonary vessels, TN-C and Prx1 expression was dramatically expanded in the smooth muscle cells of the vascular lesion as well as cells surrounding the lesion (Fig. 4N and P). We also detected strongly elevated TN-C and Prx1 expression in the pulmonary vasculature of one *Smad8*^{laz} $+/-$ mouse. As noted earlier, this finding in *Smad8* heterozygotes is consistent with the dominant genetics that is observed in human PAH patients.

Elevated phospho-Smad2 immunoreactivity in *Smad8* deficient pulmonary vessels

A balanced interplay between Activin/Tgfβ and Bmp-signaling has been recognized to be important in developing embryos (36,37). Moreover, smooth muscle cells from a PAH patient have been shown to have altered response to Tgfβ signaling (38–40). Moreover, upregulated Tgfβ signaling has been implicated in the abnormal vascular morphogenesis and maintenance observed in Marfan's syndrome (41). We examined the status of Activin/Tgfβ signaling in *Smad8* mutant pulmonary vessels using an antibody against phospho-Smad2 (P-Smad2). Our findings indicate that in the control, there are rare P-Smad2 positive cells while in the *Smad8* mutant vessels, P-Smad2 immunoreactivity is dramatically upregulated (Fig. 5A–D). We conclude that Activin/Tgfβ signaling is upregulated in *Smad8* mutant pulmonary vessels.

Lung adenomas in *Smad8* deficient mice

During our characterization of the adult lung phenotypes, we noted that a percentage of *Smad8* mutants had pulmonary tumors. Gross inspection of dissected lungs followed by histologic analysis revealed that 3 out of 19 adult *Smad8*^{laz} $-/-$ mice had lung tumors (16%) (Fig. 6A and B). Sectioning through the adenomas revealed a well-differentiated papillary histopathology (Fig. 6C–E). We next performed PCNA staining on *Smad8*^{laz} $-/-$ adenomas and control counterparts. In the adenomas, we estimated that 80–90% was PCNA positive indicating a loss-of-growth control in the absence of *Smad8*. In the *Smad8*^{laz} $+/-$ lungs, PCNA positive cells were accounted for ~40% of the lung parenchyma (Fig. 6C–E). Taken together, these finding indicate that *Smad8* plays a role in restricting cell proliferation in lung parenchyma.

Table 1. Genotype of Smad8^{ex4,5} mice at embryonic timepoints

Stages(dpc)	+/+	+/−	−/−	Total
7.5	5	11	10	26
10.5	6	22	5	33
13.5	11	17	15	43
Total	22	50	30	102

P-value = 0.129.

Table 2. Genotype of postnatal Smad8^{lacZ} or Smad8^{ex4,5} mice

	+/+	+/−	−/−	Total
Smad8^{ex4,5}	37	55	32	124
Smad8^{lacZ}	33	57	17	107
Total	70	112	49	231

P-value = 0.163.

DISCUSSION

Although the involvement of *BmpRII* in PAH is firmly established, a clear picture of the signaling pathways downstream of *BmpRII* is lacking. Previous work, documenting mutations in *BmpRII* in patients with familial PAH, established a requirement for Bmp-signaling in pulmonary vessel homeostasis. However, because BmpRII can signal via both Smad-dependent and Smad-independent pathways, a firm connection to Smad function and PAH was lacking in the whole animal. Our data show that *Smad8* has a role in regulating abnormal pulmonary vascular remodeling. *Smad8* mutant lungs had aberrant expression of Prx1 and enhanced Activin/Tgfβ-signaling. Taken together, our data extend the understanding of the genetic pathways involved in PAH.

Smad8 mutant mice as a model for human PAH

ECM remodeling is one of the most common characteristics of PAH in human patients. Other common pathologic findings include pulmonary artery wall thickening and inflammation. In *Smad8* mutant mice, we observed a number of pathologic hallmarks associated with human PAH, including ECM remodeling, arterial wall thickening and peri-vascular inflammatory infiltrates. Moreover, these changes are associated with upregulation of the *Prx1*-dependent TN-C expression, a marker of pathologic ECM remodeling, that has been previously described in human PAH samples (34,42,43). Notably, the pathologic pulmonary vascular changes in *Smad8* mutant mice were incompletely penetrant. Incomplete penetrance, in which some family members are asymptomatic carriers, is also commonly seen in familial cases of PAH and has been interpreted to represent the influence of secondary factors such as environmental insults and genetic background.

One important difference between the *Smad8* mutant model and human patients was the time to disease onset. Whereas the human patients tend to present early in life, the *Smad8* mutants developed disease relatively late in life. Experimental models often use hypoxia or other noxious stimuli while the *Smad8* mutants in this study were housed at sea level (Houston, Texas) and were unchallenged. In addition, our analysis used primarily male mice, whereas PAH predominantly afflicts female human patients. Together, these considerations support the general notion that a second insult is required for the development of symptomatic disease in humans.

Our preliminary findings, looking at pulmonary vascular resistance in *Smad8* mutants, indicate that there are no significant changes in *Smad8* mutants ($n = 4$) although more mice will need to be examined. Together, our findings reveal that *Smad8* mutant mice are a unique, single gene inactivation model for mild PAH.

Bmp signaling in vascular remodeling

Development of the pulmonary vasculature is a special case of vascular development as angiogenesis and vasculogenesis progress independently (44). The proximal vessels develop via angiogenic sprouting from the dorsal aorta, while the distal lung vasculature forms through inductive interactions in the foregut mesoderm. During vascular development, signaling from endothelium to mesenchyme is thought to be important for the recruitment of supporting cells, such as smooth muscle precursors and pericytes, that are important for the stabilization of the forming endothelial tubes (45–47). Vascular remodeling involves local disruption of the critical interaction between endothelium and support cells resulting in endothelial regression and vascular remodeling. *Bmp4*, likely signaling through the type I Bmp receptor, *Bmpr1a*, has been implicated in vascular remodeling during development (15,48). In addition, *Bmp2* is also known to be critical for cushion and valve morphogenesis during cardiac development (26).

It is conceivable that a *Smad8* regulated pathway directly constrains abnormal vascular remodeling. However, upregulated P-Smad2 implicates crosstalk with Activin/Tgfβ signaling in *Smad8* mutant pathologic remodeling. Moreover, TN-C is known to play a direct role in vascular proliferation and remodeling suggesting that this pathway has a role in *Smad8* mutants (43). It is notable that Prx1, a TN-C transcriptional regulator, is also likely to have an important role in the *Smad8* mutant phenotype as *Prx1* mutant mice have abnormal pulmonary vascular development (35). *Prx1* also has a role in the differentiation and migration of smooth muscle cells (49–51) and *Prx1* can activate ECM genes in hepatic stellate cells (52). Further experiments will be necessary to dissect the individual contributions of these genes to the *Smad8* mutant phenotype.

Smad dependent and independent signaling and PAH

In vitro studies, using isolated pulmonary artery smooth muscle cells from patients with PAH, indicated that abnormal smooth muscle cell proliferation was an important factor in the etiology of PAH (39). Other work showed that inhibition of Smad and upregulation of p38 MAP kinase signaling resulted in elevated smooth muscle cell proliferation (53). Together, these findings suggest that both Smad-dependent and Smad-independent Bmp-signaling have a role in PAH.

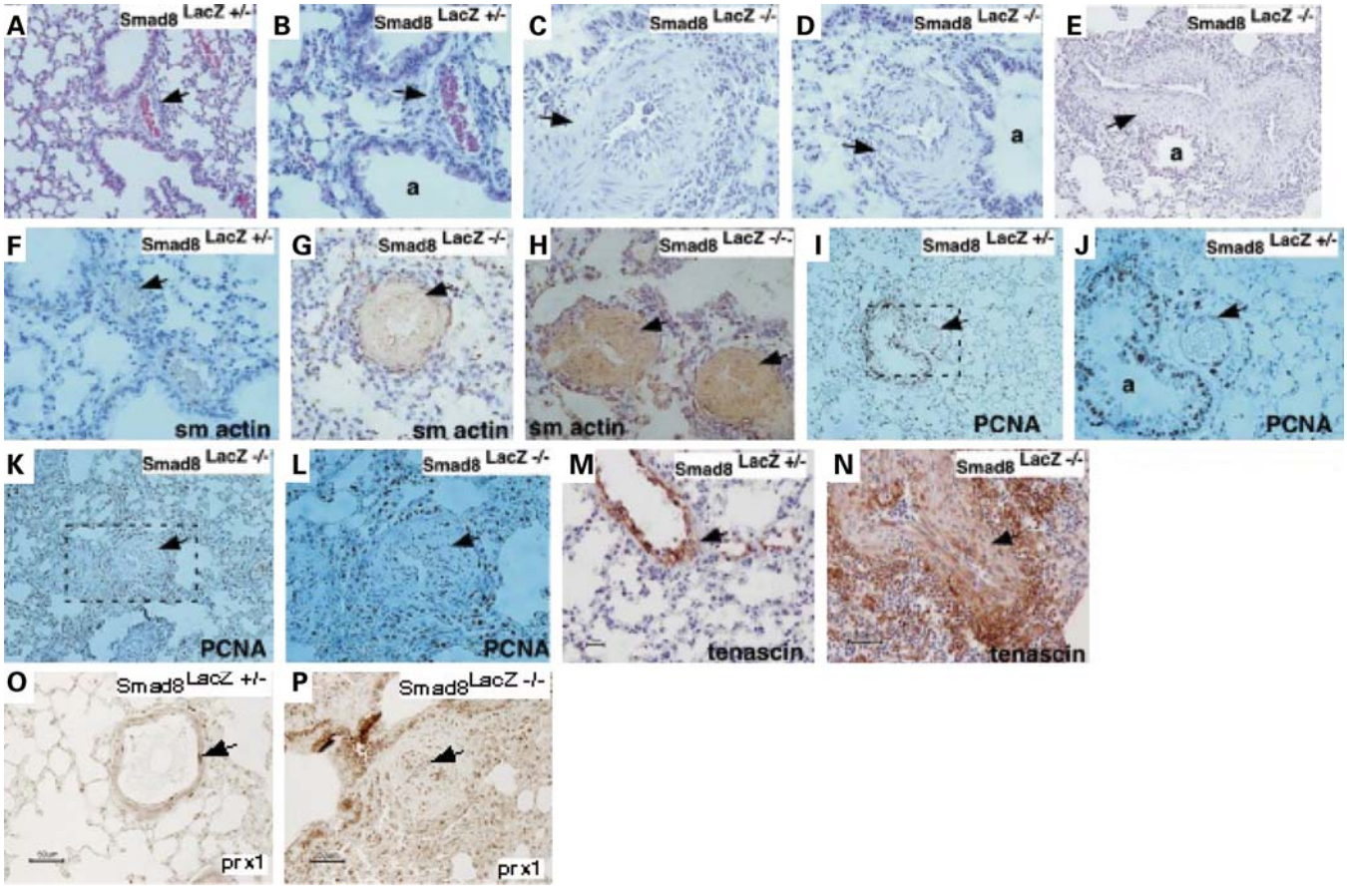

Figure 4. Abnormal pulmonary vessels in adult *Smad8* mutant mice. (**A** and **B**) Sections through control $Smad8^{lacZ}$ +/− adult mice. (**C**–**E**) Sections through three different $Smad8^{lacZ}$ −/− adult mice showing abnormal pulmonary vessel morphology with hyperplastic media (denoted by arrows). (**F**–**H**) Smooth muscle actin (sm actin) immunostaining on pulmonary vessels of control and *Smad8* mutant mice. (**I**–**L**) PCNA immunostaining of sections through control and mutant adult mice. (**M**–**P**) Immunostaining for TN-C and Prx1 in control and mutant vessels. The genotypes are shown and arrows denote positive signal. a, airway.

However, further complexity in *BmpRII* function was uncovered by the finding that BmpRII signals directly to the cytoskeleton. Protein interaction studies indicated that BmpRII cytoplasmic domain directly interacts with LIM kinase1, a regulator of actin dynamics (54,55). Moreover, disease causing mutations in the BmpRII cytoplasmic domain interrupt a functional interaction with a dynein motor protein, *Tctex1* (56). These data indicate that direct signaling of BmpRII to the cytoskeleton may have a role in the pathogenesis of PAH.

Our data support the conclusion that *Smad8* likely functions in the smooth muscle cells. Other data, using transgenic overexpression of a mutant *BmpRII* in smooth muscle, indicate that Bmp-signaling functions in smooth muscle (57,58). Our findings suggest that *Smad8* functions to restrain smooth muscle proliferation or migration. The hypothesis that *Smad8* is directly involved in control of proliferation is supported by our observation that many *Smad8* mutant mice develop lung adenomas that have elevated levels of proliferation. It will be important in future studies to inactivate *Smad8* specifically in pulmonary smooth muscle using the $Smad8^{flox}$ allele that we have generated to definitively investigate these ideas.

Smad8 in tumorigenesis and growth control

Bmp-signaling has been implicated in regulation of normal prostate development (59–62). Furthermore, one clinical study reported the loss of nuclear Smad8 immunostaining in human patients with prostate cancer (63). We have analyzed the prostates of Smad mutant male mice and have not detected any evidence for prostate cancer in mice aged to 17 months. Thus, if *Smad8* has a direct role in the initiation or progression of prostate cancer, other environmental or genetic insults must also be required for disease to occur. Our immunohistochemistry data indicate that Smad8 protein is localized to the cytoplasm in an inactive state (Fig. 1J–M). It may be that *Smad8* plays a role in response to injury in the prostatic epithelium. This hypothesis awaits further analysis.

Bmp-signaling has been implicated in specification of the pylorus (30,31). Moreover, mutations in *Bmpr1a* and *Smad4* have been found in patients with JPSs of the gut (4). In the adult gut, it is thought that Bmp-signaling maintains a stem-cell population within the crypt-villus axis through inhibition of Wnt signaling (64). We have not detected a propensity to form intestinal polyps in the *Smad8* mutant mice although this is ongoing work.

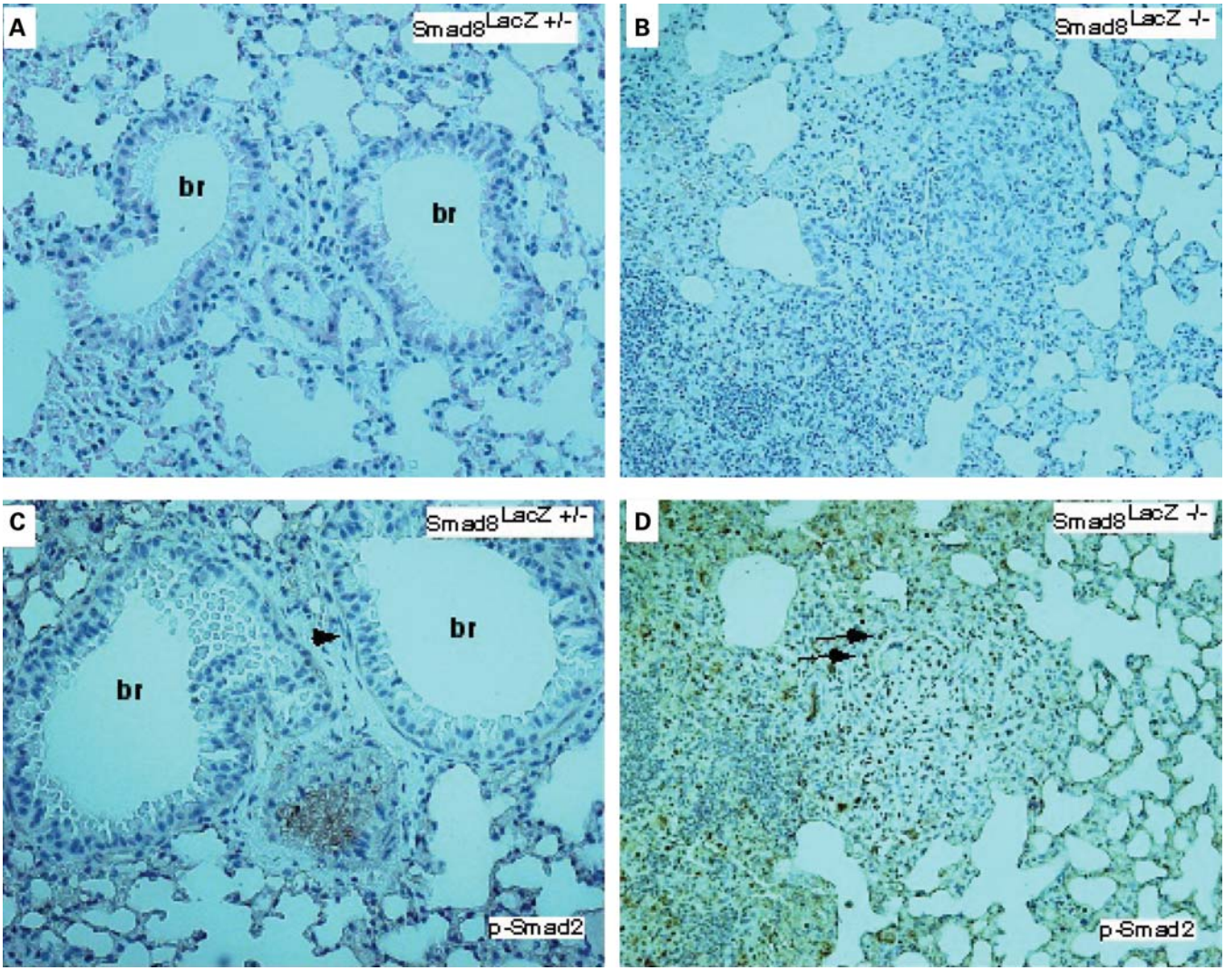

Figure 5. Expanded Activin/Tgfβ-signaling in *Smad8* mutant pulmonary vessels. (**A** and **B**) H&E staining of control and *Smad 8* mutant pulmonary vessels. (**C** and **D**) P-Smad2 immunostaining on control and *Smad8* mutant. The arrow in (C) shows P-Smad2 immunostaining in a smooth muscle cell surrounding a bronchus. In (D), the *Smad8* mutant has extensive P-Smad2 positive cells in an abnormal vascular lesion (all sections imaged at 200× magnification). br, bronchus.

Smad8 is transcriptionally regulated during development and in the adult

The analysis of the $Smad8^{lacZ}$ allele indicates that *Smad8* is regulated transcriptionally during development. Previous work established that at early stages of development, *Smad8* is expressed broadly in the embryo and then localizes to individual organs (20,23). Our data indicate that later, at stages of embryonic organogenesis and in adult organs, *Smad8* is regulated transcriptionally. Furthermore, the embryonic regions that express Smad8 are known to be areas of active Bmp-signaling. In the cardiac OFT, where high levels of *Smad8* transcription were found, we have previously shown that Bmp4-signaling plays a critical role (15). Bmp signaling is also known to be important for a specification of the pylorus, another region with $Smad8^{lacZ}$ activity.

Surprisingly, in the adult, we also found evidence for the transcriptional regulation of *Smad8* with high levels of transcription in the lung, prostate epithelium and gut. The immunostaining data in the prostate indicate that Smad8 protein is present but is localized in the cytoplasm in an inactive state (Fig. 1J–M). Taken together, our findings indicate that *Smad8*, in addition to the multiple levels of post-transcriptional regulation involved in Bmp-signaling, is also transcriptionally regulated.

The function of *Smad8* in embryogenesis

A previous report of two hypomorphic *Smad8* alleles revealed that *Smad8* may have a minor function in midbrain and hindbrain development (65). In that work, an in-frame deletion of exon 3 resulted in mice with no phenotype. A second allele, referred to as $Smad8^{3loxP}$, had a retained neomycin cassette in the intron downstream of exon 3 but no deletion of coding sequences. Due to alternative splicing, it was shown

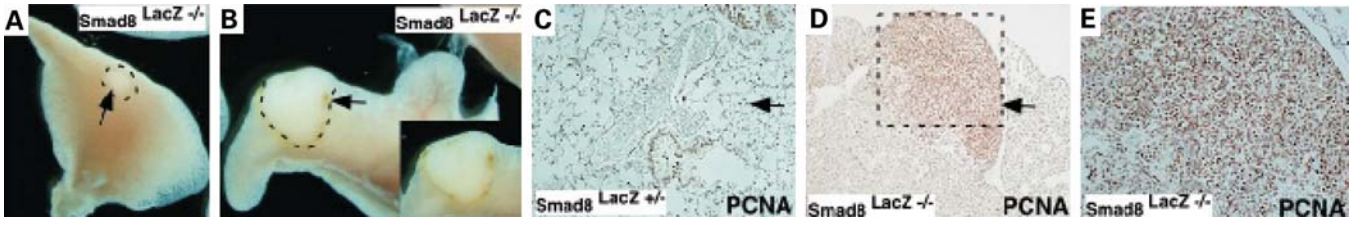

Figure 6. Lung adenomas in adult *Smad8* mutant mice. (**A** and **B**) Whole mount view of dissected lungs from $Smad8^{lacZ}$ −/− adult mice. Outlined areas with arrows denote the tumor. In (B), the inset show a close-up view of the outlined area in B. (**C**–**E**) Sections and PCNA staining through the lung of an adult $Smad8^{lacZ}$ +/− mouse and an adenoma from a $Smad8^{lacZ}$ −/− lung. The genotypes are shown and arrows denote PCNA signal.

by RT–PCR that the $Smad8^{3loxP}$ allele caused a reduction in *Smad8* expression in the brain with a potential disruption of *Smad8* exons 4 and 5. The phenotype of the homozygous mutant $Smad8^{3loxP}$ embryos was a mild midbrain and hindbrain reduction in 11% of embryos (65). Another Smad8 allelic series that included a deletion of the first coding exon failed to detect similar phenotypes. Our data also support the conclusion that Smad8 has a minor role in development likely as a result of redundancy at later stages of organogenesis. More extensive analysis using conditional genetics will be required to address this issue.

MATERIALS AND METHODS

Generation of *Smad8* mutant alleles

Screening of a 129/S mouse genomic library (Research Genetics, Inc.) using a fragment containing *Smad8* exon 3 yielded several BAC clones. Thirteen kb *Hin*dIII and 18.5 kb *Eco*RV fragments were subcloned into Bluescript SK vector, respectively. To construct the targeting vector for the $Smad8^{flox}$ allele, a LoxP and *Hin*dIII and *Bam*HI sites were placed downstream of the 3.2 kb *Bam*HI/*Xho*I 5′ arm. Another LoxP followed by Frt-flanked PGK-neo cassette was put upstream of the 0.9 kb *Hin*dIII/*Kpn*I 3′ arm. The *Pac*I linearized construct was electroporated into AK7 ES cells and G418 colonies screened by Southern blot using the 5′ external probe, a 1.4 kb fragment containing exon 3. DNA from ES cell clones screened with 5′ probe was then digested with *Bam*HI and further confirmed using 3′ external probe, a 0.5 kb *Kpn*I fragment. Six of 200 ES cells were correctly targeted and two clones contributed to the germline. To generate the $Smad8^{ex4,5}$ allele, 129 S6/S4 congenic males carrying a CMV-Cre transgene were crossed to F1 females, resulting in deletion of exons 4 and 5. The deletion was confirmed by Southern analysis using the 3′ external probe. Heterozygous offspring carrying $Smad8^{ex4,5}$ allele was backcrossed to the 129S6/S4 strain and then interbred.

The $Smad8^{lacZ}$ allele was generated by inserting an IRES LacZ/PGK-neo LoxP cassette into exon 4. The cassette was inserted into a *Sal*I site, which was introduced into exon 4 using PCR. 5′ PCR product was amplified using oligos: 5′-GCAGTCATAAGTGAGAGGCTATGGAC-3′ and 5′-TAAGTCGACCTTGAGGCTGCAGCCGCT-3′; 3′ PCR product was amplified using oligos: 5′-ATGTCGACGGCTTTGAAGTGGTGTATGAG-3′ and 5′-ATGCGGCCGCATTACAGGGAAAGAGACTCAA-3′. 5′ product was then ligated with the 3.2 kb *Bam*HI/*Xho*I 5′ arm. 3′ 3.0 kb PCR product was taken as 3′ arm for homologous recombination. The vector was linearized with *Pac*I and electroporated into AK7 ES cells, the same digest and probes as those for $Smad8^{ex4,5}$ allele were used to screen for recombinant ES clones. Two targeted ES clones were transmitted through the germline.

Genotyping of mice

F1 offspring of both alleles was genotyped by Southern analysis. Then the following generations were genotyped by PCR. DNA isolated from tail clips or yolk sac was used for genotyping. For distinction of *Smad8* wild-type and *Smad8 ex4,5* alleles, PCR was performed using 5′ common primer-A 5′-GCAGTCATAAGTGAGAGGCTATGGAC-3′ and 3′ primer-1 5′-AGAGAAGGTGCGTGTGCCCTGAATAC-3′ for wild-type allele and 3′ primer-2 5′-TAAAGCGCATGCTCCAGACTGCCTT-3′ for mutant allele, yielding 320 and 410 bp fragment, respectively. To distinguish wild-type allele and $Smad8^{lacZ}$ allele, PCR was performed using 5′ common primer-B 5′-TGCTGGGAGCTGGGCAATTTCT-3′ and 3′ primer-3 5′-AAGCTCATCCGAATCGTGCAC-3′ for wild-type allele and 3′ primer-4 5′-ATAGCTTGGCTGCAGGTCGACCTC-3′ for $Smad8^{lacZ}$ allele, yielding products of 470 and 370 bp, respectively. A single PCR program used for all genotyping tasks was: 94°C for 5 min, then 35 cycles of 94°C for 30 s, 62°C for 30 s, 72°C for 45 s, followed by an extension of 72°C for 10 min.

LacZ staining, histology and immunohistochemistry

Whole embryos and organs from adult mice were collected and fixed in fixation buffer (0.2% glutaraldehyde, 2% formaldehyde, 5 mM EGTA, 2 mM $MgCl_2$, in 0.1 M pH 7.3 phosphate-buffered saline for 30 min at room temperature). After three washes, 30 min each, in rinse buffer (0.1% sodium deoxycholate, 0.2% Nonidet P-40, 2 mM $MgCl_2$, in 0.1 M pH 7.3 phosphate-buffered saline), ß-galactosidase (LacZ) activity was detected by incubation overnight at room temperature in rinse buffer containing 1 mg/ml X-gal (5-bromo-4-chloro-3-indolyl-ß-D-galactosidase), 5 mM potassium ferricyanide and 5 mM potassium ferrocyanide. After staining, embryos and organs were rinsed in PBS twice and postfixed in 10% formaldehyde, before photography.

For histology, embryos and organs were fixed in 10% formaldehyde at 4°C overnight. After dehydration through a graded ethanol series, embryos and organs were embedded in paraffin at appropriate orientations. Paraffin blocks were

sectioned at the thickness of 5 μm. Sections were stained with hematoxylin and eosin using standard procedures.

Immunohistochemistry was performed on paraffin-embedded sections of the adult prostate tissue. Sections were deparaffinized in xylene, rehydrated through graded ethanol and heated in 95°C deionized water for 10 min. Sections were incubated with goat anti-Smad8 polyclonal antibody (catalog number: *sc-7442*, Santa Cruz Biotechnology, Inc.) or Phospho-Smad2 (catalog number: 3101, Cell Signaling Technology) at 4°C overnight and stained using goat or rabbit ABS staining system (catalog number: sc-2023, Santa Cruz Biotechnology, Inc.), then counterstained with hematoxylin. Immunostaining for Tenascin-C and Prx1 has been previously described (35). For the analysis of *Smad8* mutant pulmonary vasculature, we analyzed male mice at the ages discussed.

ACKNOWLEDGEMENTS

We thank A. Bradley, P. Soriano and R. Behringer for reagents.

Conflict of Interest statement. None declared.

FUNDING

This work was supported by grants from the NIH 2R01DE/HD12324-12, R01DE16329 to J.F.M.

REFERENCES

1. Hogan, B.L. (1996) Bone morphogenetic proteins: multifunctional regulators of vertebrate development. *Genes. Dev.*, **10**, 1580–1594.
2. Derynck, R. and Zhang, Y.E. (2003) Smad-dependent and Smad-independent pathways in TGF-beta family signalling. *Nature*, **425**, 577–584.
3. Davis, B.N., Hilyard, A.C., Lagna, G. and Hata, A. (2008) SMAD proteins control DROSHA-mediated microRNA maturation. *Nature*, **454**, 56–61.
4. Waite, K.A. and Eng, C. (2003) From developmental disorder to heritable cancer: it's all in the BMP/TGF-beta family. *Nat. Rev. Genet.*, **4**, 763–773.
5. Eng, C. (2001) To be or not to BMP. *Nat. Genet.*, **28**, 105–107.
6. Lane, K.B., Machado, R.D., Pauciulo, M.W., Thomson, J.R., Phillips, J.A., Loyd, J.E., Nichols, W.C. and Trembath, R.C. (2000) Heterozygous germline mutations in BMPR2, encoding a TGF-beta receptor, cause familial primary pulmonary hypertension. The International PPH Consortium. *Nat. Genet.*, **26**, 81–84.
7. Farber, H.W. and Loscalzo, J. (2004) Pulmonary arterial hypertension. *N. Engl. J. Med.*, **351**, 1655–1665.
8. Deng, Z., Morse, J.H., Slager, S.L., Cuervo, N., Moore, K.J., Venetos, G., Kalachikov, S., Cayanis, E., Fischer, S.G., Barst, R.J. *et al.* (2000) Familial primary pulmonary hypertension (gene PPH1) is caused by mutations in the bone morphogenetic protein receptor-II gene. *Am. J. Hum. Genet.*, **67**, 737–744.
9. Morrell, N.W. (2006) Pulmonary hypertension due to BMPR2 mutation: a new paradigm for tissue remodeling? *Proc. Am. Thorac. Soc.*, **3**, 680–686.
10. Shintani, M., Yagi, H., Nakayama, T., Saji, T. and Matsuoka, R. (2009) A new nonsense mutation of SMAD8 associated with pulmonary arterial hypertension. *J. Med. Genet*, **46**, 331–337.
11. Haramis, A.P., Begthel, H., van den Born, M., van Es, J., Jonkheer, S., Offerhaus, G.J. and Clevers, H. (2004) De novo crypt formation and juvenile polyposis on BMP inhibition in mouse intestine. *Science*, **303**, 1684–1686.
12. Howe, J.R., Bair, J.L., Sayed, M.G., Anderson, M.E., Mitros, F.A., Petersen, G.M., Velculescu, V.E., Traverso, G. and Vogelstein, B. (2001) Germline mutations of the gene encoding bone morphogenetic protein receptor 1A in juvenile polyposis. *Nat. Genet.*, **28**, 184–187.
13. Shore, E.M., Xu, M., Feldman, G.J., Fenstermacher, D.A., Cho, T.J., Choi, I.H., Connor, J.M., Delai, P., Glaser, D.L., LeMerrer, M. *et al.* (2006) A recurrent mutation in the BMP type I receptor ACVR1 causes inherited and sporadic fibrodysplasia ossificans progressiva. *Nat. Genet.*, **38**, 525–527.
14. Sapkota, G., Alarcon, C., Spagnoli, F.M., Brivanlou, A.H. and Massague, J. (2007) Balancing BMP signaling through integrated inputs into the Smad1 linker. *Mol. Cell*, **25**, 441–454.
15. Liu, W., Selever, J., Wang, D., Lu, M.F., Moses, K.A., Schwartz, R.J. and Martin, J.F. (2004) Bmp4 signaling is required for outflow-tract septation and branchial-arch artery remodeling. *Proc. Natl Acad. Sci. USA*, **101**, 4489–4494.
16. Chang, H., Huylebroeck, D., Verschueren, K., Guo, Q., Matzuk, M.M. and Zwijsen, A. (1999) Smad5 knockout mice die at mid-gestation due to multiple embryonic and extraembryonic defects. *Development*, **126**, 1631–1642.
17. Chang, H., Zwijsen, A., Vogel, H., Huylebroeck, D. and Matzuk, M.M. (2000) Smad5 is essential for left-right asymmetry in mice. *Dev. Biol.*, **219**, 71–78.
18. Yang, X., Castilla, L.H., Xu, X., Li, C., Gotay, J., Weinstein, M., Liu, P.P. and Deng, C.X. (1999) Angiogenesis defects and mesenchymal apoptosis in mice lacking SMAD5. *Development*, **126**, 1571–1580.
19. Lechleider, R.J., Ryan, J.L., Garrett, L., Eng, C., Deng, C., Wynshaw-Boris, A. and Roberts, A.B. (2001) Targeted mutagenesis of Smad1 reveals an essential role in chorioallantoic fusion. *Dev. Biol.*, **240**, 157–167.
20. Tremblay, K.D., Dunn, N.R. and Robertson, E.J. (2001) Mouse embryos lacking Smad1 signals display defects in extra-embryonic tissues and germ cell formation. *Development*, **128**, 3609–3621.
21. Beppu, H., Kawabata, M., Hamamoto, T., Chytil, A., Minowa, O., Noda, T. and Miyazono, K. (2000) BMP type II receptor is required for gastrulation and early development of mouse embryos. *Dev. Biol.*, **221**, 249–258.
22. Mishina, Y., Suzuki, A., Ueno, N. and Behringer, R.R. (1995) Bmpr encodes a type I bone morphogenetic protein receptor that is essential for gastrulation during mouse embryogenesis. *Genes. Dev.*, **9**, 3027–3037.
23. Arnold, S.J., Maretto, S., Islam, A., Bikoff, E.K. and Robertson, E.J. (2006) Dose-dependent Smad1, Smad5 and Smad8 signaling in the early mouse embryo. *Dev. Biol.*, **296**, 104–118.
24. Orvis, G.D., Jamin, S.P., Kwan, K.M., Mishina, Y., Kaartinen, V.M., Huang, S., Roberts, A.B., Umans, L., Huylebroeck, D., Zwijsen, A. *et al.* (2008) Functional redundancy of TGF-beta family type I receptors and receptor-Smads in mediating anti-Mullerian hormone-induced Mullerian duct regression in the mouse. *Biol. Reprod.*, **78**, 994–1001.
25. McCulley, D.J., Kang, J.O., Martin, J.F. and Black, B.L. (2008) BMP4 is required in the anterior heart field and its derivatives for endocardial cushion remodeling, outflow tract septation, and semilunar valve development. *Dev. Dyn.*, **237**, 3200–3209.
26. Ma, L., Lu, M.F., Schwartz, R.J. and Martin, J.F. (2005) Bmp2 is essential for cardiac cushion epithelial-mesenchymal transition and myocardial patterning. *Development*, **132**, 5601–5611.
27. Jiao, K., Kulessa, H., Tompkins, K., Zhou, Y., Batts, L., Baldwin, H.S. and Hogan, B.L. (2003) An essential role of Bmp4 in the atrioventricular septation of the mouse heart. *Genes. Dev.*, **17**, 2362–2367.
28. Li, Y., Gordon, J., Manley, N.R., Litingtung, Y. and Chiang, C. (2008) Bmp4 is required for tracheal formation: a novel mouse model for tracheal agenesis. *Dev. Biol.*, **322**, 145–155.
29. Que, J., Choi, M., Ziel, J.W., Klingensmith, J. and Hogan, B.L. (2006) Morphogenesis of the trachea and esophagus: current players and new roles for noggin and Bmps. *Differentiation*, **74**, 422–437.
30. Smith, D.M., Nielsen, C., Tabin, C.J. and Roberts, D.J. (2000) Roles of BMP signaling and Nkx2.5 in patterning at the chick midgut-foregut boundary. *Development*, **127**, 3671–3681.
31. Theodosiou, N.A. and Tabin, C.J. (2005) Sox9 and Nkx2.5 determine the pyloric sphincter epithelium under the control of BMP signaling. *Dev. Biol.*, **279**, 481–490.
32. Jones, P.L. and Rabinovitch, M. (1996) Tenascin-C is induced with progressive pulmonary vascular disease in rats and is functionally related to increased smooth muscle cell proliferation. *Circ. Res.*, **79**, 1131–1142.
33. Chapados, R., Abe, K., Ihida-Stansbury, K., McKean, D., Gates, A.T., Kern, M., Merklinger, S., Elliott, J., Plant, A., Shimokawa, H. *et al.* (2006)

ROCK controls matrix synthesis in vascular smooth muscle cells: coupling vasoconstriction to vascular remodeling. *Circ. Res.*, **99**, 837–844.
34. Ihida-Stansbury, K., McKean, D.M., Lane, K.B., Loyd, J.E., Wheeler, L.A., Morrell, N.W. and Jones, P.L. (2006) Tenascin-C is induced by mutated BMP type II receptors in familial forms of pulmonary arterial hypertension. *Am. J. Physiol. Lung Cell Mol. Physiol.*, **291**, L694–L702.
35. Ihida-Stansbury, K., McKean, D.M., Gebb, S.A., Martin, J.F., Stevens, T., Nemenoff, R., Akeson, A., Vaughn, J. and Jones, P.L. (2004) Paired-related homeobox gene prx1 is required for pulmonary vascular development. *Circ. Res.*, **94**, 1507–1514.
36. Candia, A.F., Watabe, T., Hawley, S.H., Onichtchouk, D., Zhang, Y., Derynck, R., Niehrs, C. and Cho, K.W. (1997) Cellular interpretation of multiple TGF-beta signals: intracellular antagonism between activin/BVg1 and BMP-2/4 signaling mediated by Smads. *Development*, **124**, 4467–4480.
37. Furtado, M.B., Solloway, M.J., Jones, V.J., Costa, M.W., Biben, C., Wolstein, O., Preis, J.I., Sparrow, D.B., Saga, Y., Dunwoodie, S.L. *et al.* (2008) BMP/SMAD1 signaling sets a threshold for the left/right pathway in lateral plate mesoderm and limits availability of SMAD4. *Genes. Dev.*, **22**, 3037–3049.
38. Long, L., Crosby, A., Yang, X., Southwood, M., Upton, P.D., Kim, D.K. and Morrell, N.W. (2009) Altered bone morphogenetic protein and transforming growth factor-beta signaling in rat models of pulmonary hypertension: potential for activin receptor-like kinase-5 inhibition in prevention and progression of disease. *Circulation*, **119**, 566–576.
39. Morrell, N.W., Yang, X., Upton, P.D., Jourdan, K.B., Morgan, N., Sheares, K.K. and Trembath, R.C. (2001) Altered growth responses of pulmonary artery smooth muscle cells from patients with primary pulmonary hypertension to transforming growth factor-beta(1) and bone morphogenetic proteins. *Circulation*, **104**, 790–795.
40. Phillips, J.A. 3rd, Poling, J.S., Phillips, C.A., Stanton, K.C., Austin, E.D., Cogan, J.D., Wheeler, L., Yu, C., Newman, J.H., Dietz, H.C. *et al.* (2008) Synergistic heterozygosity for TGFbeta1 SNPs and BMPR2 mutations modulates the age at diagnosis and penetrance of familial pulmonary arterial hypertension. *Genet. Med.*, **10**, 359–365.
41. Neptune, E.R., Frischmeyer, P.A., Arking, D.E., Myers, L., Bunton, T.E., Gayraud, B., Ramirez, F., Sakai, L.Y. and Dietz, H.C. (2003) Dysregulation of TGF-beta activation contributes to pathogenesis in Marfan syndrome. *Nat. Genet.*, **33**, 407–411.
42. Jones, P.L., Crack, J. and Rabinovitch, M. (1997) Regulation of tenascin-C, a vascular smooth muscle cell survival factor that interacts with the alpha v beta 3 integrin to promote epidermal growth factor receptor phosphorylation and growth. *J. Cell. Biol.*, **139**, 279–293.
43. Jones, F.S. and Jones, P.L. (2000) The tenascin family of ECM glycoproteins: structure, function, and regulation during embryonic development and tissue remodeling. *Dev. Dyn.*, **218**, 235–259.
44. Dettman, R.W. and Steinhorn, R.H. (2004) Connecting the cells: vascular differentiation via homeobox genes and extracellular matrix in the distal lung [In Process Citation]. *Circ. Res.*, **94**, 1406–1407.
45. Hanahan, D. (1997) Signaling vascular morphogenesis and maintenance. *Science*, **277**, 48–50.
46. Yancopoulos, G.D., Davis, S., Gale, N.W., Rudge, J.S., Wiegand, S.J. and Holash, J. (2000) Vascular-specific growth factors and blood vessel formation. *Nature*, **407**, 242–248.
47. Cleaver, O. and Melton, D.A. (2003) Endothelial signaling during development. *Nat. Med.*, **9**, 661–668.
48. Park, C., Lavine, K., Mishina, Y., Deng, C.X., Ornitz, D.M. and Choi, K. (2006) Bone morphogenetic protein receptor 1A signaling is dispensable for hematopoietic development but essential for vessel and atrioventricular endocardial cushion formation. *Development*, **133**, 3473–3484.
49. Shang, Y., Yoshida, T., Amendt, B.A., Martin, J.F. and Owens, G.K. (2008) Pitx2 is functionally important in the early stages of vascular smooth muscle cell differentiation. *J. Cell. Biol.*, **181**, 461–473.
50. Jin, L., Kern, M.J., Otey, C.A., Wamhoff, B.R. and Somlyo, A.V. (2007) Angiotensin II, focal adhesion kinase, and PRX1 enhance smooth muscle expression of lipoma preferred partner and its newly identified binding partner palladin to promote cell migration. *Circ. Res.*, **100**, 817–825.
51. Jones, F.S., Meech, R., Edelman, D.B., Oakey, R.J. and Jones, P.L. (2001) Prx1 controls vascular smooth muscle cell proliferation and tenascin-C expression and is upregulated with Prx2 in pulmonary vascular disease. *Circ. Res.*, **89**, 131–138.
52. Jiang, F. and Stefanovic, B. (2008) Homeobox gene Prx1 is expressed in activated hepatic stellate cells and transactivates collagen alpha1(I) promoter. *Exp. Biol. Med. (Maywood)*, **233**, 286–296.
53. Yang, X., Long, L., Southwood, M., Rudarakanchana, N., Upton, P.D., Jeffery, T.K., Atkinson, C., Chen, H., Trembath, R.C. and Morrell, N.W. (2005) Dysfunctional Smad signaling contributes to abnormal smooth muscle cell proliferation in familial pulmonary arterial hypertension [In Process Citation]. *Circ. Res.*, **96**, 1053–1063.
54. Foletta, V.C., Lim, M.A., Soosairajah, J., Kelly, A.P., Stanley, E.G., Shannon, M., He, W., Das, S., Massague, J., Bernard, O. *et al.* (2003) Direct signaling by the BMP type II receptor via the cytoskeletal regulator LIMK1. *J. Cell Biol.*, **162**, 1089–1098.
55. Lee-Hoeflich, S.T., Causing, C.G., Podkowa, M., Zhao, X., Wrana, J.L. and Attisano, L. (2004) Activation of LIMK1 by binding to the BMP receptor, BMPRII, regulates BMP-dependent dendritogenesis. *EMBO J.*, **23**, 4792–4801.
56. Machado, R.D., Rudarakanchana, N., Atkinson, C., Flanagan, J.A., Harrison, R., Morrell, N.W. and Trembath, R.C. (2003) Functional interaction between BMPR-II and Tctex-1, a light chain of Dynein, is isoform-specific and disrupted by mutations underlying primary pulmonary hypertension. *Hum. Mol. Genet.*, **12**, 3277–3286.
57. West, J., Fagan, K., Steudel, W., Fouty, B., Lane, K., Harral, J., Hoedt-Miller, M., Tada, Y., Ozimek, J., Tuder, R. *et al.* (2004) Pulmonary hypertension in transgenic mice expressing a dominant-negative BMPRII gene in smooth muscle. *Circ. Res.*, **94**, 1109–1114.
58. West, J., Harral, J., Lane, K., Deng, Y., Ickes, B., Crona, D., Albu, S., Stewart, D. and Fagan, K. (2008) Mice expressing BMPR2R899X transgene in smooth muscle develop pulmonary vascular lesions. *Am. J. Physiol. Lung Cell Mol. Physiol.*, **295**, L744–L755.
59. Kim, I.Y., Lee, D.H., Lee, D.K., Ahn, H.J., Kim, M.M., Kim, S.J. and Morton, R.A. (2004) Loss of expression of bone morphogenetic protein receptor type II in human prostate cancer cells. *Oncogene*, **23**, 7651–7659.
60. Haudenschild, D.R., Palmer, S.M., Moseley, T.A., You, Z. and Reddi, A.H. (2004) Bone morphogenetic protein (BMP)-6 signaling and BMP antagonist noggin in prostate cancer. *Cancer Res.*, **64**, 8276–8284.
61. Kim, I.Y., Lee, D.H., Ahn, H.J., Tokunaga, H., Song, W., Devereaux, L.M., Jin, D., Sampath, T.K. and Morton, R.A. (2000) Expression of bone morphogenetic protein receptors type-IA, -IB and -II correlates with tumor grade in human prostate cancer tissues. *Cancer Res.*, **60**, 2840–2844.
62. Lamm, M.L., Podlasek, C.A., Barnett, D.H., Lee, J., Clemens, J.Q., Hebner, C.M. and Bushman, W. (2001) Mesenchymal factor bone morphogenetic protein 4 restricts ductal budding and branching morphogenesis in the developing prostate. *Dev. Biol.*, **232**, 301–314.
63. Horvath, L.G., Henshall, S.M., Kench, J.G., Turner, J.J., Golovsky, D., Brenner, P.C., O'Neill, G.F., Kooner, R., Stricker, P.D., Grygiel, J.J. *et al.* (2004) Loss of BMP2, Smad8 and Smad4 expression in prostate cancer progression. *Prostate*, **59**, 234–242.
64. He, X.C., Zhang, J., Tong, W.G., Tawfik, O., Ross, J., Scoville, D.H., Tian, Q., Zeng, X., He, X., Wiedemann, L.M. *et al.* (2004) BMP signaling inhibits intestinal stem cell self-renewal through suppression of Wnt-beta-catenin signaling. *Nat. Genet.*, **36**, 1117–1121.
65. Hester, M., Thompson, J.C., Mills, J., Liu, Y., El-Hodiri, H.M. and Weinstein, M. (2005) Smad1 and smad8 function similarly in Mammalian central nervous system development. *Mol. Cell Biol.*, **25**, 4683–4692.